Optical and radiation shielding properties for novel glass material: $TeO_2/Nb_2O_5/Ta_2O_5/La_2O_3$

K. I. Hussein[a,b,*], F. F. Alqahtani[c], M. S. Alqahtani[a,d], K. J. Alzahrani[a], H. Y. Zahran[e,f], A. M. Alshehri[e], I. S. Yahia[e,f,g], M. Reben[h], A. M. Alqahtani[i], E. Yousef[e,f]

[a]*Department of Radiological Sciences, College of Applied Medical Sciences, King Khalid University, Abha 61421, Saudi Arabia.*
[b]*Department of Medical Physics and Instrumentation, National Cancer Institute, University of Gezira, Wad Medani 2667, Sudan.*
[c]*Department of Radiological Sciences, College of Applied Medical Sciences, Najran University, Najran 1988, Saudi Arabia.*
[d]*BioImaging Unit, Space Research Centre, Department of Physics and Astronomy, University of Leicester, Leicester LE1 7RH, UK.*
[e]*Physics Department, Faculty of Science, King Khalid University, Postcode: 9004, Zip code: 61413, Abha, Saudi Arabia*
[f]*Research Center for Advanced Materials Science (RCAMS), King Khalid University, Postcode: 9004, Zip code: 61413, Abha, Saudi Arabia*
[g]*Nanoscience Laboratory for Environmental and Bio-Medical Applications (NLEBA), Semiconductor Lab., Metallurgical Lab. 2 Physics Department, Faculty of Education, Ain Shams University, Roxy, 11757 Cairo, Egypt*
[h]*Faculty of Materials Science and Ceramics, AGH – University of Science and Technology, al. Mickiewicza 30, 30-059 Cracow, Poland.*
[i]*Medical and Clinical Affairs Department, King Faisal Medical City, Abha 62523, Saudi Arabia*

Glass samples with (86-x)TeO_2 – 12Nb_2O_5- x(Ta_2O_5) -1.0La_2O_3 where x = 1.0 (glass TNTL1), 5.0 (glass TNTL2), 8.0 (glass TNTL3), and 10 (glass TNTL4) mol% composition were synthesized by a melt quenching technique. The gamma-ray attenuation parameters of TNTL system such as MAC, LAC, HVL, MFP, Z_{eff}, and N_{eff} were analyzed in this study in order to better understand the effect of Ta_2O_5 on photon absorption.Within the 190-2500-nm wavelength range, the optical properties of prepared TNTL glasses were also evaluated. It was observed from the optical absorption spectra that all glass samples studied had good optical transparency. The findings indicated that adding Ta_2O_5 to glass enhances the gamma protection ability as well as the optical properties. The densities of the samples ranged from 5.66 to 6.49 g/cm3, depending on the Ta2O5 concentration. Sample TNTL4 had the best preformace, according to the results recorded.

(Received March 19, 2022; Accepted June 14, 2022)

Keywords: Oxide glasses, Refractive index, Energy gap, Gamma shielding

1. Introduction

Shielding against ionizing radiation is based on the idea of reducing or eliminating any negative effects on the population. One of the most commonly used gamma rays is used in nuclear research centers, radiotherapy and medical equipment sterilization. Medical professionals, patients, and others who come into contact with gamma photon sources need to be protected from the harm

[*] Corresponding author: kirahim@kku.edu.sa
https://doi.org/10.15251/CL.2022.196.417

that these photons can cause [1-3]. Radiation-protection materials have been developed using a wide range of novel materials, including lead and concrete. The primary function of these materials is to shield humans from harmful radiation [2, 3]. Lead has a number of drawbacks, including low mechanical strength and toxicity, according to current research. Nuclear and substance engineers and researchers are working on developing new shielding materials to reduce harmful radiation [4–6]. Radiation shielding glass, on the other hand, is becoming increasingly popular. As a result, glass materials, such as X-ray rooms, CT scans, and other imaging systems, can be used to create doors and windows in medical and nuclear facilities. Because of their unique mechanical and physical properties (such as hardness, improved corrosion resistance, and ease of production in a variety of methods), glasses are becoming more popular with scientists. Glasses have a wide range of fascinating properties, including high attenuation, excellent optical transparency, and strong mechanical and thermal properties, particularly in samples containing heavy metal oxides. In order to achieve an adequate level of safety, the glass composition must be modified as little as possible [10-14]. Heavy metal oxide (HMO) glass, which contains lead, tellurite, bismuth, and antimony, has a wide range of unusual properties, including high electrical conductivity, high solubility of rare-earth ions, high infrared transmissivity, and a wide optical bandwidth. For example, HMO-based glass has a higher shielding capacity than ordinary glass [15–17]. In order to create a variety of different types of glass, additional oxides can be added to the host glass system. Innovations in high-strength, structurally stable glasses have led to an increase in the popularity of glasses over the past few decades. Because of the development of structurally stable glasses with high radiation shielding capabilities, the usage of glasses as radiation shields has continued to rise. In addition, the fabrication of glass materials and the measurement of their radiation shielding properties have continued to grow in popularity among researchers and material scientists throughout the world. There are also many parameters that can be used to determine the gamma-ray attenuation attributes of any glass system, the most important of which are the mass attenuation coefficient (MAC), linear attenuation coefficient, effective atomic number, tenth-value layer, mean free path, electron density, and half-value layer [18–20]. In the present work, the radiation shielding characteristics and optical properties of glass system with the composition of (86-x) TeO_2 –$12Nb_2O_5$- x(Ta_2O_5) -1.0La_2O_3 (Where x = 1.0, 5.0, 8.0, and 10 mol%) were investigated. Furthermore, the prepared glasses were compared with some standard material

2. Experiment work

Glasses with the compositions (86-x)TeO_2 – $12Nb_2O_5$- x(Ta_2O_5) -1.0La_2O_3, where x = 1.0 (glass TNTL1), 5.0 (glass TNTL2), 8.0 (glass TNTL3), and 10 (glass TNTL4) mol%. The raw materials were put in a platinum crucible at 900 °C, and then cast in a graphite mould. The fabricated glasses were annealing at 320 °C for 2hr. Then the furnace switched off and allowed to cool. The radiation shielding parameters used to charterized the shielding effeciency of the prepared glasses were calculated using new developed software MIKE [21].

3. Results and Discussion

3.1. Optical investigations

A single monochromator UV-Visible-Near Infrared spectrophotometer with a resolution of 2 nm in the wavelength range of 190–2500 nm was used to analyze the optical absorption spectra of the produced glasses. Fig. 1 shows absorbance against wavelength in the 300–2500 nm range. As shown in Fig. 1, in the wavelength (λ) range from 300 nm to 600 nm, there is a significant decrease in absorbance. As from Fig. 1, it is shown that there is no sharp absorption edge in the spectra, which confirms the amorphous nature of TNTL samples.

The optical refractive index was determined using ellipsometry data acquired with an M-2000 Woollam ellipsometer. The ability to use the prepared glasses (TNTL1-TNTL4) in optical applications is mostly determined by the optical refractive index. As a result, n was calculated for all prepared glasses. Equation 1 was used to calculate the refractive index (n) for indirect allowed transitions in the Tauc model. Table 1 lists the n values for the investigated samples. The value of the optical energy band gaps was inversely proportional to the refractive indices of the samples studied. Since the value of all glasses was high (about 2.19), the prepared glasses can be used as potential photocell and optical filter devices. At 479 nm, n rises from 2.1281 to 2.2083 as the doped ion concentration rises from 1.0 to 10%. The refractive index is influenced by a variety of variables, including: (i) the coordination number of the doping ions, (ii) the polarizability of the first adjacent ions (anion), (iii) the density of the component substance, and (vi) the bulk glasses' optical basicity. The refractive index in direct and indirect allowed transitions is calculated using Equations [22, 23]:

$$\left(\frac{n^2-1}{n^2+1}\right) = 1 - \left(\frac{E_{BAND}}{20}\right)^{0.5} \tag{1}$$

The glass samples' densities were determined using Archimedes' Principle by the following equation:

$$\rho = \left(\frac{W_a}{W_a - W_l}\right)\rho_l \tag{2}$$

where $(\rho, \rho_l, w_a,\ w_l)$ are the density of the glass sample, the density of toluene, the weight of the glass sample in air and the weight of the glass sample in toluene, respectively. The density of toluene is 0.865 g/cm^3 with an error of ± 0.005. Table 1 shows the density values of the prepared glasses.

The values of molar volume, V_m, the molar volume of oxygen, V_o, and oxygen packing density, $O.P.D.$, were calculated using equations the following equations:

$$V_m = \frac{\sum i x_i m_i}{\rho} \tag{3}$$

$$V_o = (V_m).\left(\frac{1}{x_i n_i}\right) \tag{4}$$

$$O.P.D. = \sum i \frac{1000.\rho.n_i}{m_i} \tag{5}$$

where, (x_i, m_i, n_i) is the molar fraction of every oxide compound, the molecular weight of the glassy structure, and the number oxygen atoms of each oxide.

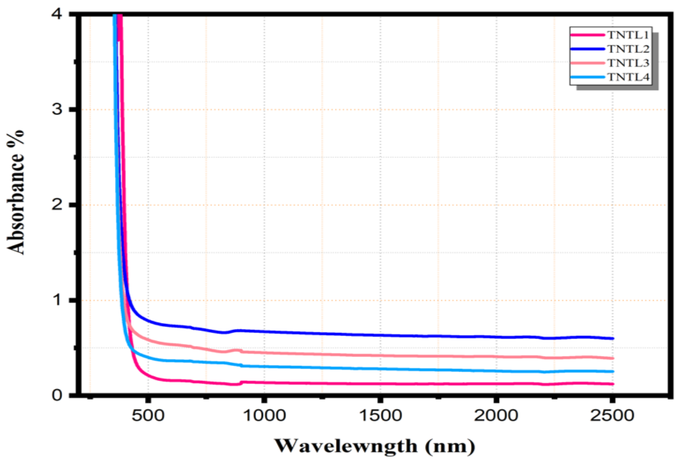

Fig. 1. Absorbance spectroscopy of different compositions of TNTL.

When the Ta_2O_5 ions concentration increased from 1.0 to 10 mol%, the density increases from 5.892 to 6.1221 g/cm3 as shown in Table 1. Similarly, as shown in Table 2, V_m have increased from 30.01 to 33.03 cm^3 and V_O have decreased from 12.50 to 12.37 cm^3 mol^{-1} in relation to the oxygen spatial distributions in the glass matrix. Otherwise, increasing the Ta_2O_5 concentration from 1.0 to 10 mol percent raises the O.P.D. value from 79.97 to 80.83 gm atm L^{-1}. The Molecular weight, number of oxygen atoms, bond lengths, and the cation radius and coordination number all affect V_m and V_O. When interpreting changes in V_m and V_O, these factors must be taken into account. The molecular weight and coordination numbers of glass composition, as well as cross-link density, are the factors that affecting the density of glass system.

Table 1. Chemical compositions of prepared glasses in mol% doped with Ta_2O_5 concentration, density, and refractive Index.

Glass sample code	**Composition (mol%)**				**Density**	**Refrective index**
	TeO_2	**Nb_2O_5**	**Ta_2O_5**	**La_2O_3**		
TNTL1	86	12	1.0	1.0	5.8921	2.1281
TNTL2	82	12	5.0	1.0	5.9745	2.1513
TNTL3	79	12	8.0	1.0	6.0316	2.1827
TNTL4	77	12	10	1.0	6.1221	2.2083

Table 2.The V_m, oxygen molar volume, V_o, optical packing density, $O.p.d$, energy gap E_{opt}, Urbach energy, ΔE, of glass.

Sample code	Vm	V0 ($cm^3.mol^{-1}$)	OPD ($cm^3.Mol^{-1}$)	Energy gap, Eopt, in (eV)	Urbach energy ΔE, in eV
TNTL1	30.01	12.59	79.97	2.791	0.351
TNTL2	31.49	12.49	80.03	2.912	0.576
TNTL3	32.59	12.48	80.07	3.048	0.449
TNTL4	33.03	12.37	80.83	3.105	0.408

The following formula [24,25] is used to determine the optical band gap.

$$(\alpha h\nu)^n = A(h\nu - E_g) \qquad (6)$$

A is a constant, E_g is the optical band gap, $h\nu$ is the energy of the incident spectrum, and α is the absorption coefficient.

Moreover, n describes the transition process whose value is equal to 2 in the case of a direct allowed transition. On the other hand, if n equal to 1/2, it is related to an indirect allowed transition as shown in Fig. 2.

As shown in Table 2, the value of E_{opt} depends mainly on the Ta_2O_5 ions concentration doped in the host glasses. It increases from 2.912 to 3.105 eV when increasing Ta_2O_5 from 5.0 to 10 mol% in the host matrix. The Urbach energy is considered to be a measure of disorder in the glasses. According to Tauc, transitions from the non-bridging oxygen (NBO), which has a less firmly bound electron than bridging oxygen (BO), correlate to a shift in the absorption band to lower energy. As a result, it can be deduce that the growing quantity of NBO is causing a decrease in the energy gap of sample TNTL1. Furthermore, because of its small energy gap, sample TNTL1 can be considered as an excellent semiconducting material. In amorphous materials, there exists a band tailing in the forbidden energy band gap.

The Urbach energy was computed by using following relation which defines the width of band tails [26].

$$\ln(\alpha) = \ln(\alpha_0) + \frac{h\nu}{E_U} \qquad (7)$$

The α and α0 are the absorption coefficient and constant, respectively; denoted by, and the E_u is the Urbach energy. The E_u values are obtained by plotting $ln(\alpha)$ versus $h\nu$ and calculating the adverse slope for the curves as shown in Fig. 3. The E_u values of the prepared glasses increased as the Ta_2O_5 concentration increased as represented in Table 3. The glass with composition of $77TeO_2 - 12Nb_2O_5 - 10Ta_2O_5 - 1.0La_2O_3$ has highest value with ΔE= 0.4080 eV, while $86TeO_2 - 12Nb_2O_5 - 1.0Ta_2O_5 - 1.0La_2O_3 - 1.0mol\ Ta_2O_5$ has lowest value ΔE = 0 .3516 eV. As a result, glass with lower Urbach energies have a lower risk of bond breakage and defect creation. This implies that the glasses under investigation have a good homogenous nature.

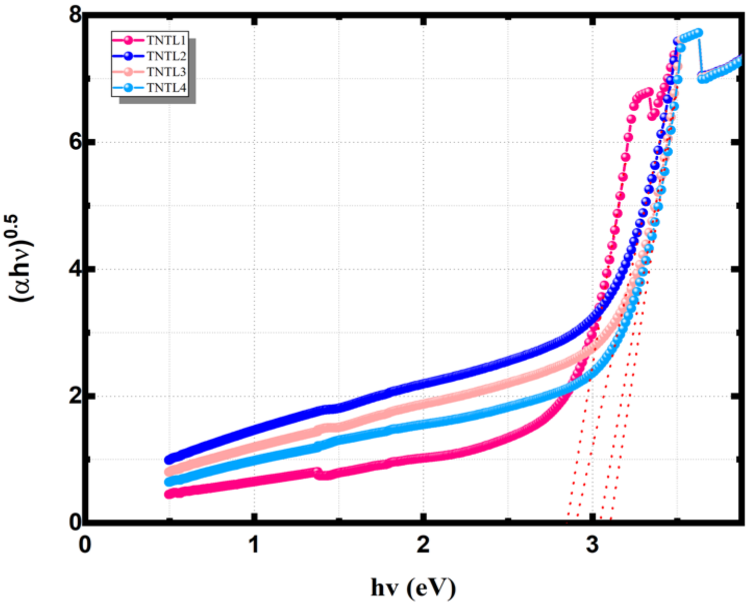

Fig. 2. Spectral dependence of ln $(\alpha h\nu)^{1/2}$, and hν in eV for prepared glasses.

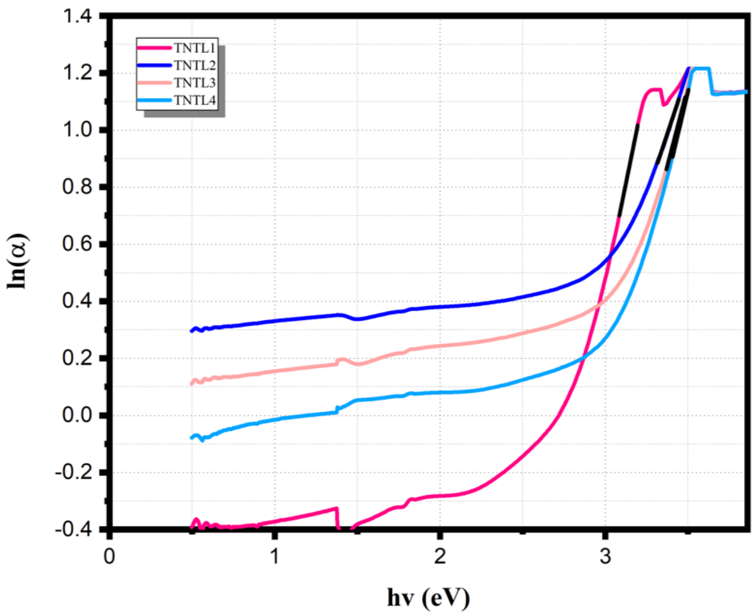

Fig. 3. Spectral dependence of ln (α), and hν in eV for prepared glasses.

The molar refraction, R_m, molar polarizability, α_m, and the metallization criterion, M_c, were calculated using equations (8), (9), and (10).

$$R_m = V_m . \frac{n^2-1}{n^2+2} \quad (8)$$

$$\alpha_m = \frac{3}{4\pi N_A V_m} \cdot (\frac{n^2-1}{n^2+2})^{-1} \quad (9)$$

$$M_c = 1 - \frac{n^2-1}{n^2+2} \quad (10)$$

The R_m and α_m values are increased from 16.22 to 18.62 $cm^3\ mol^{-1}$ (from 6.43 to 7.38 A^{03}) with increasing doped Ta_2O_5 from 1.0 to 10 mol% in the host TNTL1 glasses. Table 3. summarizes these findings. In the present work, we discovered that the refractive index value strongly depends on the ratio α_m/V_m (i.e., the n value increases with increasing ratio α_m/V_m).

Table 3. The molar reflection, R_m, electronic polarizability, α_m,of the studied glasses.

Glass sample code	**Molar polarizability, α_m, (Å^3)**	**Molar refraction, R_m, (cm^3/mol)**
TNTL1	6.4369	16.2211
TNTL2	6.8395	17.2356
TNTL3	7.1975	18.1378
TNTL4	7.3898	18.6224

3.2. Gamma shielding properties

The gamma ray shielding is dependent on the value of mass attenuation coefficient, which can be determined using the Beer–Lambert law [25, 26]:

$$I = I_0 e^{-\mu x} \quad (11)$$

where, x, μ, I and I_0 denote to thickness, linear attenuation coefficient, and the intensities of the transmitted and incident photon beams, respectively. MIKE software [21] was used to calculate theoretical MAC values for the glasses from their constituent elements based on the mixing rule [25, 26]:

$$\mu_m = \left(\frac{\mu}{\rho}\right) = \sum i\, w_i (\frac{\mu}{\rho})_i \quad (12)$$

AS shown in Fig. 4 the shielding characteristics of the glasses (86-x) TeO_2 –$12Nb_2O_5$-x(Ta_2O_5) -1.0La_2O_3 (Where x = 1.0, 5.0, 8.0, and 10 mol%) were illustrated for energy ranging 0.015 MeV to 15 MeV. As shown in Fig. 4a, the MAC values of all samples decreased rapidly as photon energy increased up to 0.2 MeV due to the dominance of the photoelectric process but stayed almost constant between 1MeV to 3MeV due to the dominance of Compton scattering. The values of MAC then slowly increase, which may be attributed to the pair production process. The discontinuities in MAC curve can be seen at the low energy range at the K-edge of Nb at 20.67 keV, due to the effect of photoelectric absorption.

Additionally, as the TeO_2 concentration declined from 86 to 77 mol % as shown in Fig. 4, the MAC values reduced from 52.90 to 0.03617 cm^2/g at 10MeV. Furthermore, it is seen that the substitution of TeO_2 with Ta_2O_5 causes a decrease in the MAC values. For the present glass system, the calculated MAC values increase in the order TNTL4 > TNTL3 < TNTL2 > TNTL1. Finally, it should be noted that the greatest MAC values are found in TNTL4 and TNTL3 glasses, which means that they offer the best protection against gamma radiation. This may be explained by the fact that TNTL3 and TNTL4 glasses possess a high concentration of Ta_2O_5 (8.0 mol% TNTL3, 10 mol% TNTL4), which is also correlates to the highest densities values.

The linear attenuation coefficient (LAC) is frequently used to describe and differentiate gamma photon penetration through glasses and other shielding materials.The MIKE programe was used to evaluate the LAC TNTL glass system with various amount of Ta_2O_3. Fig. 4b depicts the energy dependence of the LAC for the samples under investigation. The of values of LAC decreases rapidly with increasing energy, and this is due to a variety of photon interactions [27].

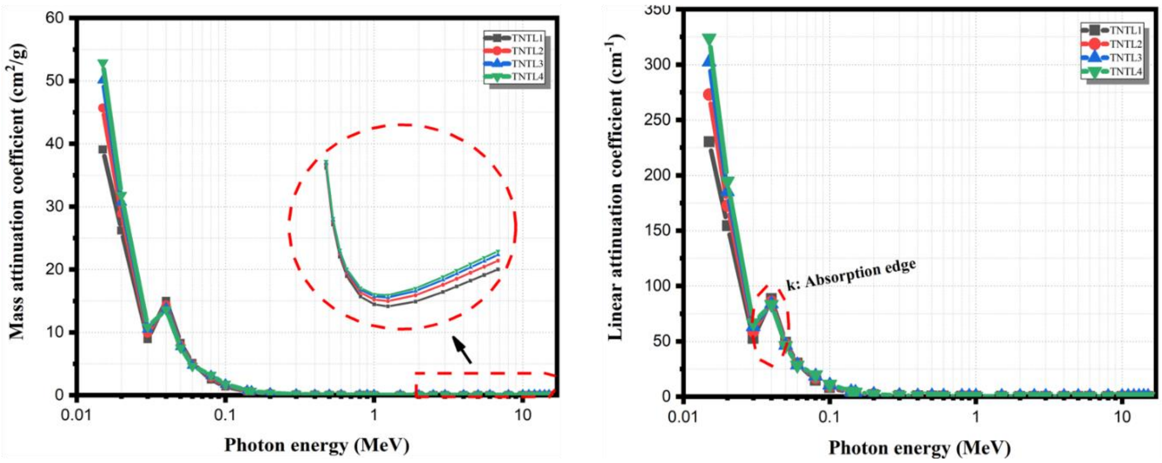

(a) *(b)*

Fig.4. (a) Mass attenuation coefficients MAC (b) Linear attenuation coefficients of the prepared glasses at photon energy from 0.015 to 15 MeV.

A material's radiation shielding capabilities are primarily indicated by the half-value layer (HVL), tenth values layer (TVL), and mean free path (MFP), which are all considered critical gamma-ray shielding parameters. These parameters can be determined using the following equations [28, 29]:

$$HVL = \frac{\ln(2)}{\mu} = \frac{0.693}{\mu}(cm) \tag{13}$$

$$TVL = \frac{\ln(10)}{LAC_\mu} = \frac{2.302}{LAC_\mu}(cm) \tag{14}$$

$$MFP = \frac{1}{LAC_\mu}(cm) \tag{15}$$

The HVL and TVL and MFP are illustrated in fig. 5 a, b and c. As shown in Fig. 5, the calculated HVL, TVL, and MFP values have the lowest values at low energies. The values of HVL, TVL, and MFP increase as the energy increases, reaching their highest values at 5 MeV. The variations in LAC values for known glass samples can be explained by the dominance of different photon interaction types in different energy zones. Additionally, these values drop as the density of the glass samples increases. For a preferred gamma ray shielding material, low MFP, HVL, and TVL values are needed because the likelihood of photon interaction with the material is higher when these values are low. The TNTL4 glass sample has the lowest HVL, TVL, and MFP, as well as the highest density and mass attenuation coefficient, when compared to the other glass samples. As a result, it provides excellent protection of any of the glass analyzed samples The prepared samples were compared to other standard concrete materials such as barite, chromite, magnetite, ferrite, and commercial glass materials such as RS-253-G18, RS-360, and RS-520). As shown in Fig. 6 a and b the prepared samples recoded the lowest HVL and MFP compared to all standard materials at the energy range under investigation. The standard material that contains the highest concentration of lead oxide (71%) has slightly better performance than the prepared.

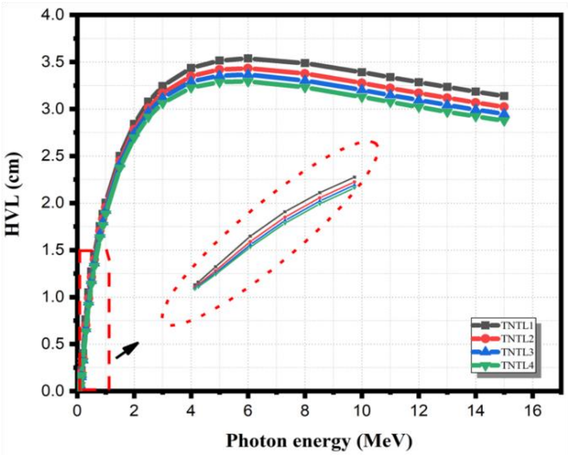

(a)

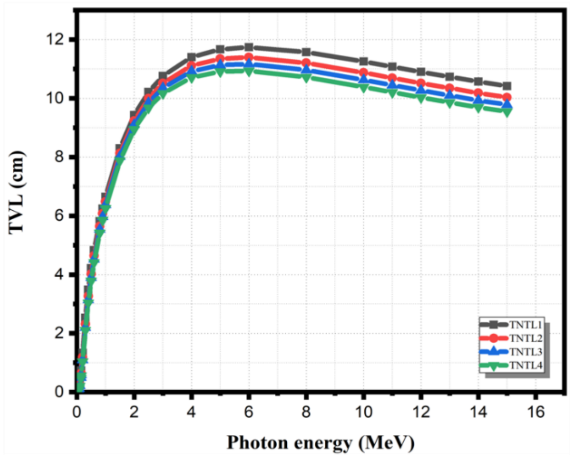

(b)

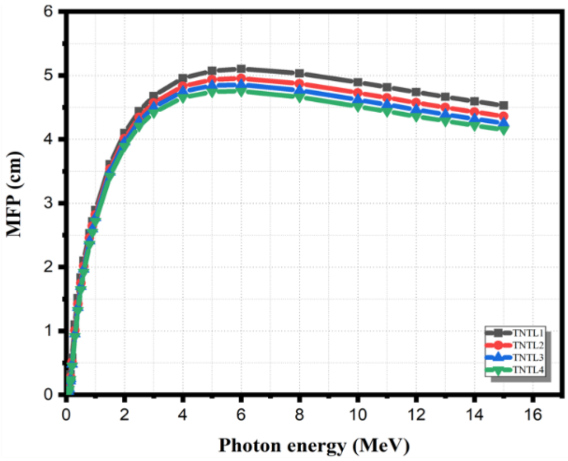

(c)

Fig. 5 (a) The half-value layer (b) The tenth -value layer (c) The mean free path of prepared glasses.

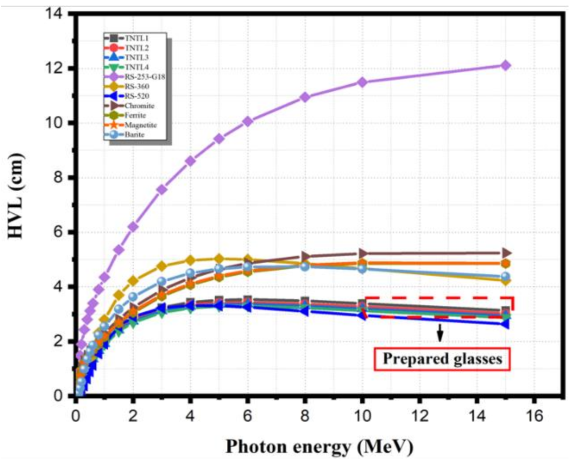

(a)

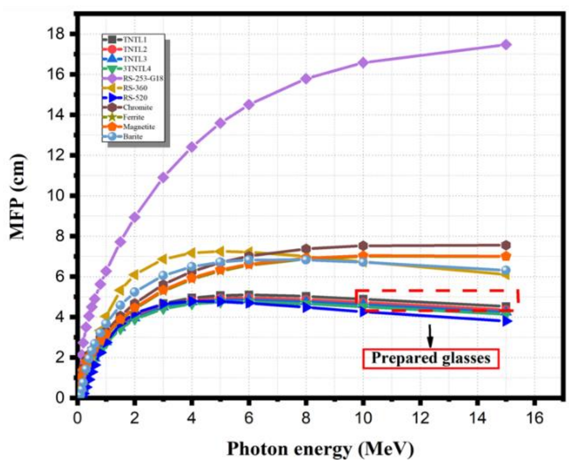

(b)

Fig. 6 (a) The half layer values (HVLs) (b) Mean free path of the investigated glass systems compared with standard materials.

The photon interaction with the TNTL glasses system can aslo be described by the effective atomic number (Zeff) and Neff, which presents the number of electrons per unit mass. Neff, which is closely related to Z eff, can be calculated using the following equation [32]:

$$Z_{eff} = \frac{\sigma_a}{\sigma_e} \tag{16}$$

$$Z_{eff} = \frac{\sum i f_i A_{i(\mu\rho)_i}}{\sum j f_j \frac{A_j}{Z_j} (\mu\rho)_j} \tag{17}$$

$$N_{eff} = \frac{(\mu/\rho)_h}{\sigma_e} = \frac{N_A}{M} Z_{eff} \sum i\, n_i \; (electrons/g) \tag{18}$$

The Z_{eff} values for TNTL glass systems are shown in Fig. 7a. The N_{eff} values of the prepared samples derived from the Z_{eff} are shown in Fig.7b. Figure 7 shows a rapid increase in Z_{eff} at energy of 0.09 MeV as the concentration of Ta_2O_5 in glass structures is increased. This is due to the dependency of photon interaction of the atomic number of the shielding material at lower range, where the photoelectric absorption is dominant (Z^4). A significant decrease in Z_{eff} values occurs in the 0.09 MeV - 0.2 MeV range. As photon energy increases, the Z_{eff} becomes virtually independent of the energy. There is a gradual rise in the value of Z_{eff} when it crosses the threshold of 2.0 MeV, which indicates the presence of pair production. TNTL4 sample has the highest Z_{eff} value, while TNTL1 scored the lowest values.

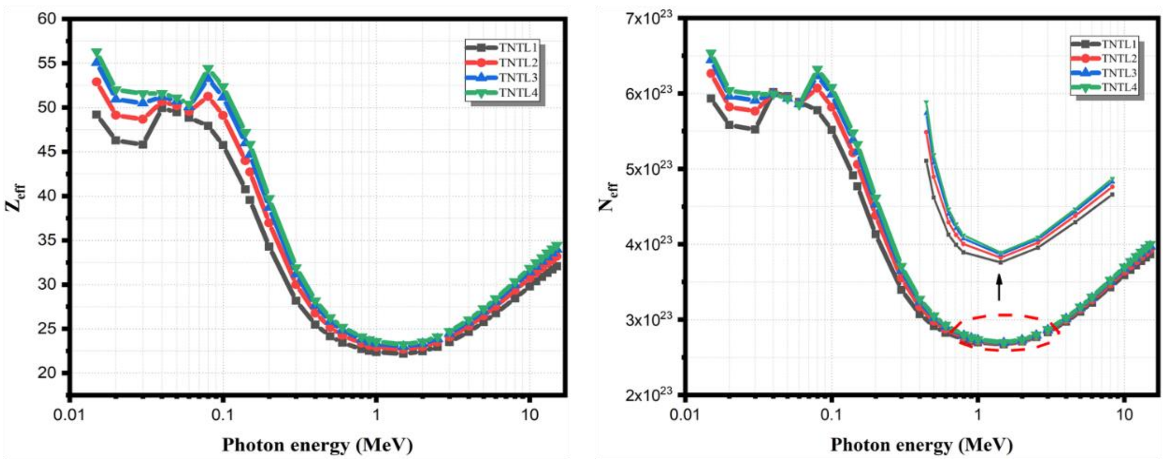

Fig. 7. Effective electron density (Nel) of the glass samples with photon energy.

4. Conclusion

Four glass systems composition of $(86-x)\,TeO_2 - 12Nb_2O_5 - (x)Ta_2O_5 - 1.0La_2O_3$,) (where x =1.0, 5.0, 8.0 and 10 mol%) were synthesized using a quenching melt procedure. Density, molar volume, and UV–Vis measurements were preformed for the prepared glasses. Moreover, the photon attenuation performance was investigated using the MIKE software. The results indicated that the MAC values are greatly affected by the Ta_2O_5 concentration and the energy. The acquired findings indicate that, of the examined glasses, the TNTL4 glass sample with a Ta_2O_5 concentration of 10% mol% exhibits superior gamma-ray shielding performance due to its higher MAC and the lower HVL and MFP. Furthermore, The investgated glasses were compared to standard materials. Except the RS-520 glass that contain the highest concentration of lead oxide, the TNTL1–TNTL4 glass samples exhibit lower HVL and MFP values than all standard materials. The prepared glasses were found to have good optical properties such as transparent to visible light, in addition to the high shielding effciency, which make them suitable candidates for many applications in medical and industrial.

Acknowledgments

The authors extend their appreciation to the Deanship of Scientific Research at Najran University for funding this work under the Research Collaboration Funding program grant code (NU/RC/MRC/11/3). Furthermore, The authors are thankful to the Deanship of Scientific Research at King Khalid University (KKU) for funding this research project Number (R.G.P2/79/41).

References

[1] Y. Elmahroug, M. Almatari, M.I. Sayyed, M. Dong, H.O. Tekin, Journal of Non-Crystalline Solids. (2018); https://doi.org/10.1016/j.jnoncrysol.2018.07.008

[2] S.S. Obaid, M.I. Sayyed, D.K. Gaikwad, H.O. Tekin, Y. Elmahroug, P.P. Pawar, Radiation Effects and Defects in Solids. 173 (2018) 900-914; https://doi.org/10.1080/10420150.2018.1505890

[3] R. Bagheri, A.K. Moghaddam, S. Pezhman Shirmardi, B. Azadbakht, M.H. Salehi, Journal of Non-Crystalline Solids. 479 (2018) 62-71; https://doi.org/10.1016/j.jnoncrysol.2017.10.006

[4] R. Bagheri, A. Khorrami Moghaddam, H. Yousefnia, Gamma Ray Shielding Nuclear Engineering and Technology. 49 (2017) 216-223; https://doi.org/10.1016/j.net.2016.08.013

[5] N. Chanthima, J. Kaewkhao, Annals of Nuclear Energy. 55 (2013) 23-28; https://doi.org/10.1016/j.anucene.2012.12.011

[6] D.K. Gaikwad, M.I. Sayyed, S.S. Obaid, S.A.M. Issa, P.P. Pawar, Journal of Alloys and Compounds. (2018); https://doi.org/10.1016/j.jallcom.2018.06.240

[7] Y. Rammah, M.S. Al-Buriahi, A.S. Abouhaswa, Physica B-Condensed Matter. 576 (2020) 411717; https://doi.org/10.1016/j.physb.2019.411717

[8] M.S. Al-Buriahi, A.S. Abouhaswa, H.O. Tekin, C. Sriwunkum, F.I. El-Agawany, T. Nutaro, E. Kavaz, Y.S. Rammah, Structure, optical, Ceramics International. 46 (2020) 1711-1721; https://doi.org/10.1016/j.ceramint.2019.09.144

[9] S. Souto, M. Massot, M. Balkanski, D. Royer, Materials Science and Engineering: B. 64 (1999) 33-38; https://doi.org/10.1016/S0921-5107(99)00150-6

[10] V.P. Singh, N.M. Badiger, N. Chanthima, J. Kaewkhao, Radiation Physics and Chemistry. 98 (2014) 14-21; https://doi.org/10.1016/j.radphyschem.2013.12.029

[11] A.E. Ersundu, M. Büyükyz, M. Elikbilek Ersundu, E. Bakar, M. Kurudirek, Progress in Nuclear Energy. 104 (2017) 280-287; https://doi.org/10.1016/j.pnucene.2017.10.008

[12] A.M. El-Khayatt, A.M. Ali, V.P. Singh, Detectors and Associated Equipment. (n.d.) 207-212; https://doi.org/10.1016/j.nima.2013.09.027

[13] M.G. Dong, O. Agar, H.O. Tekin, O. Kilicoglu, K.M. Kaky, M.I. Sayyed, Composites Part B: Engineering. 165 (2019) 636-647; https://doi.org/10.1016/j.compositesb.2019.02.022

[14] D.K. Gaikwad, M.I. Sayyed, S.N. Botewad, S.S. Obaid, Z.Y. Khattari, U.P. Gawai, F. Afaneh, M.D. Shirshat, P.P. Pawar, Journal of Non-Crystalline Solids. 503-504 (2019) 158-168; https://doi.org/10.1016/j.jnoncrysol.2018.09.038

[15] S.A. Tijani, S.M. Kamal, Y. Al-Hadeethi, M. Arib, M.A. Hussein, S. Wageh, L.A. Dim, Journal of Alloys and Compounds. 741 (2018) 293-299; https://doi.org/10.1016/j.jallcom.2018.01.109

[16] A.M. Zoulfakar, A.M. Abdel-Ghany, T.Z.A. Abou-Elnasr, A.G. Mostafa, S.M. Salem, H.H. El-Bahnaswy, Industry and Medicine. 127 (2017) 269-274; https://doi.org/10.1016/j.apradiso.2017.05.007

[17] A. Kumar, R. Kaur, M.I. Sayyed, M.M. Rashad, M. Singh, A.M. Ali, Physica B: Condensed Matter. (2019); https://doi.org/10.1016/j.physb.2018.10.001

[18] A. M. Alqahtani, M. S. Alqahtani, K. I. Hussein, A. J. Alkuli , F.F. Alqahtani, E. Yousef, Chalcogenide Letters 18 (2021) 513 - 523.

[19] D.K. Gaikwad, S.S. Obaid, M.I. Sayyed, R.R. Bhosale, V. v Awasarmol, A. Kumar, M.D. Shirsat, P.P. Pawar, Materials Chemistry and Physics. 213 (2018) 508-517; https://doi.org/10.1016/j.matchemphys.2018.04.019

[20] M.I. Sayyed, H.C. Manjunatha, D.K. Gaikwad, S.S. OBaid, M.H.M. Zaid, K.A. Matori, Digest J. Nanomater. Biostructures 13, 701-712 (2018)

[21] Hussein, K.I., Alqahtani, M.S., Algarni, H., Zahran, I.S., Yaha, I., Grelowska, M., Reben and Yousef, E.S. Mike, Journal of Instru-mentation 2021, 16, T07004; https://doi.org/10.1088/1748-0221/16/07/T07004

[22] M. Rashad, A.A.A. Darwish, Materials Research Express. 5 (2018) 26402; https://doi.org/10.1088/2053-1591/aa9ef3

[23] Y. Rammah, E.M. Awad, Radiation Physics and Chemistry. 146 (2018) 42-46; https://doi.org/10.1016/j.radphyschem.2018.01.004

[24]. M. Rashad, R. Amin, M.M. Hafz, Chalcogenide Lett. 12, 441-451 (2015).

[25] R. Mirji, B. Lobo, Radiation Physics and Chemistry. 135 (2017) 32-44; https://doi.org/10.1016/j.radphyschem.2017.03.001

[26] M.I. Sayyed, Y.S. Rammah, F. Laariedh, A.S. Abouhaswa, T.-B. Badeche, Applied Physics A. 125 (2019) 649; https://doi.org/10.1007/s00339-019-2958-1

[27] R. El-Mallawany, M.I. Sayyed, M.G. Dong, Y.S. Rammah, Radiation Physics and Chemistry. 151 (2018) 239-252; https://doi.org/10.1016/j.radphyschem.2018.06.035

[28] H.O. Tekin, E.E. Altunsoy, E. Kavaz, M.I. Sayyed, O. Agar, M. Kamislioglu, Results in Physics. 12 (2019) 1457-1464; https://doi.org/10.1016/j.rinp.2019.01.060

[29] A.M. Abu El-Soad, M.I. Sayyed, K.A. Mahmoud, E. Şakar, E.G. Kovaleva, Applied Radiation and Isotopes. 154 (2019) 108882; https://doi.org/10.1016/j.apradiso.2019.108882

[30] J.E. Ngaile, C.B.S. Uiso, P. Msaki, R. Kazema, Radiation Protection Dosimetry. 130 (2008) 490-498; https://doi.org/10.1093/rpd/ncn095

[31] V. Dimitrov, S. Sakka, Journal of Applied Physics. 79 (1996) 1736-1740; https://doi.org/10.1063/1.360962

[32] R. El-Mallawany, M.D. Abdalla, I.A. Ahmed, Materials Chemistry and Physics. 109 (2008) 291-296; https://doi.org/10.1016/j.matchemphys.2007.11.040

[33] A.E. Ersundu, M. Büyükyıldız, M. Çelikbilek Ersundu, E. Şakar, M. Kurudirek, Progress in Nuclear Energy. 104 (2018) 280-287; https://doi.org/10.1016/j.pnucene.2017.10.008